DWDM Source Based on Monolithic Side-Wall Sample Grating DFB Laser Array

Lianping Hou[1,*], Junjie Xu[2], Iain Eddie[3], Liangshun Han[2], Hongliang Zhu[2], John H. Marsh[1]

[1]*School of Engineering, University of Glasgow, Glasgow, G12 8LT, U.K.*
[2]*Institute of Semiconductor, Chinese Academy of Sciences, No. A35, East Qinghua Road, Haidian District, Beijing 1000083, P.R. China*
[3]*CST Global Ltd., 4 Stanley Blvd, Blantyre, Glasgow, G72 0BN U.K.*
**Corresponding author: lianping.hou@glasgow.ac.uk*

Abstract: We report side-wall sampled grating and quantum well intermixing techniques to fabricate a full function 4-channel DWDM source with excellent wavelength precision (residuals <0.13 nm) and high yield. Output power was >10 mW.
OCIS codes: (140.3490) Distributed-feedback lasers; (140.3290) Laser array; (230.3120) Integrated optics device.

Monolithic arrays of lasers as sources for dense wavelength division multiplexing (DWDM) are considered to be the most promising approach for the next-generation high-speed optical communication systems because of their small size, low energy consumption, and high reliability [1]. The multi-wavelength distributed feedback (DFB) laser array offers stable and highly reliable operation of each laser in a single longitudinal mode (SLM) [2]. However, one major challenge is precisely controlling the grating period Λ to give the exact Bragg wavelength: $\lambda_B=2\times n_{eff}\times\Lambda$, where n_{eff} is the effective index of the propagating mode. For example, assuming n_{eff}=3.2, steps of only 0.125 nm in Λ are needed to give a 0.8 nm spacing in λ_B, and fabrication to this tolerance is beyond the typical resolution of 0.5 nm of electron beam lithography (EBL). A second challenge is obtaining SLM operation of every laser with high yield, a challenge which can only be solved by simplifying the whole fabrication process. In this work, we use simple, flexible and low-cost techniques, based on the reconstruction equivalent chirp (REC) approach to increase the SLM yield [3] and quantum well intermixing (QWI) to realize passive waveguides.

To implement the REC approach in DFB lasers, we have used ridge waveguides with sampled gratings etched into the side-walls. The gratings for all the lasers are of the same pitch, while the operating wavelengths are determined by varying the sampling period. In the center of the DFB cavity we have modified the sampling to give an equivalent phase shift (EPS) of a quarter wavelength, an approach which substantially increases the SLM yield [3]. We have used QWI to increase the bandgap of the passive waveguide sections post-growth and so eliminated complicated and time-consuming regrown butt-joint or selective-area growth techniques. In this way, we have integrated monolithically four channels (CH) of AlGaInAs/InP DFB lasers operating at 1.55 μm with a wavelength spacing of 0.8 nm, four electroabsorption modulators (EAMs), a 41 multimode-interference (MMI) coupler, and a semiconductor optical amplifier (SOA). The epitaxial structure and fabrication processes are similar to those described in [4].

An optical micrograph and the dimensions of the device are shown in Fig. 1(a). The separation between two adjacent lasers was set at 125 μm. The ridge width was 2.5 μm. The passive section includes the S-bends and the MMI which were blue-shifted by 100 nm using QWI. The raised cosine S-bends were 1020 μm-long. The MMI coupler was 30 μm-wide and 532 μm-long (Fig. 1(d)). The 790 μm-long SOA was designed as a curved waveguide terminating at an angle of 10° relative to the normal direction of the facet. Each of the four channel DFB lasers had a total length of 1155 μm. The grating period (Λ) was 232 nm to give a 0^{th} order Bragg wavelength at 1.480 μm; this was intentionally designed to be far away from the gain peak of the quantum well active layer at ~1.55 μm to avoid lasing in the 0^{th} order mode (see Fig. 2(a)). The sampled grating periods Z_0 were set to 4.717, 4.764, 4.811, 4.858 μm for CHl to CH4 respectively, so that the 1^{st} order Bragg reflections would lie in the operating wavelength region around 1.55 μm. The sampling periods were chosen to give a wavelength spacing of 0.8 nm (see Fig. 2(a) below). The sample burst was of first-order with a 50% duty cycle (Z_1=Z_0/2) and formed by etching recesses of depth

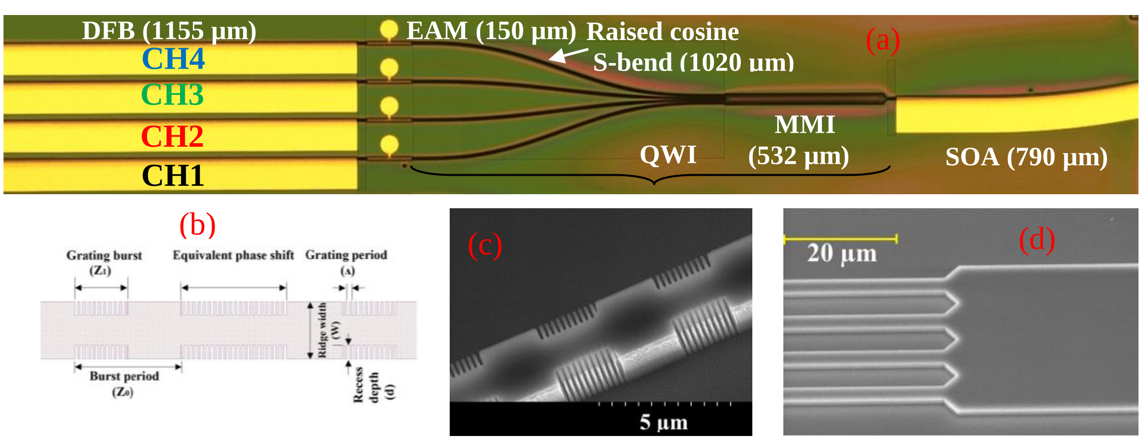

Fig1. (a) Optical micrograph of the overall laser array, (b) schematic of the side-wall sample grating with EPS, (c) SEM picture of the side-wall sample gratings, (d) input to MMI coupler section.

d = 0.6 μm into the sidewalls of the waveguide (Fig. 1(c)). The coupling coefficient of an unsampled grating, κ_0, was measured to be approximately 80 cm^{-1} using the sub-threshold spectral fitting method. The λ/4 EPS was inserted at the center of the cavity of each DFB laser (Fig. 1(b)). The EAM had a length of 150 μm, capable of encoding data at >5 Gb/s in each channel.

Fig. 2(a) shows the simulated power reflectivity of the sampling gratings of the four channel DFB lasers, taking into account the internal loss of 15/cm. The 0th order wavelength is set to be 1480 nm, and the +1st order reflection peaks determine the operating wavelengths of the lasers (from 1556.54 to 1554.14 nm with a spacing of 0.8 nm). The measured threshold currents of the four channel DFB lasers are around 100 mA. Fig. 2(b) shows the optical spectra measured at 20 °C from the SOA side with I_{DFB}=300 mA (3×I_{th}), I_{SOA}=150 mA, and V_{EAM}=0 V. The peak wavelengths of the four channels were at 1558, 1557.27, 1556.62, 1555.64 nm with a wavelength spacing around 0.8 nm, nearly the same as the simulated results in Fig. 2(a) except that the measured wavelengths experienced a redshift due to the higher injection current (300 mA).

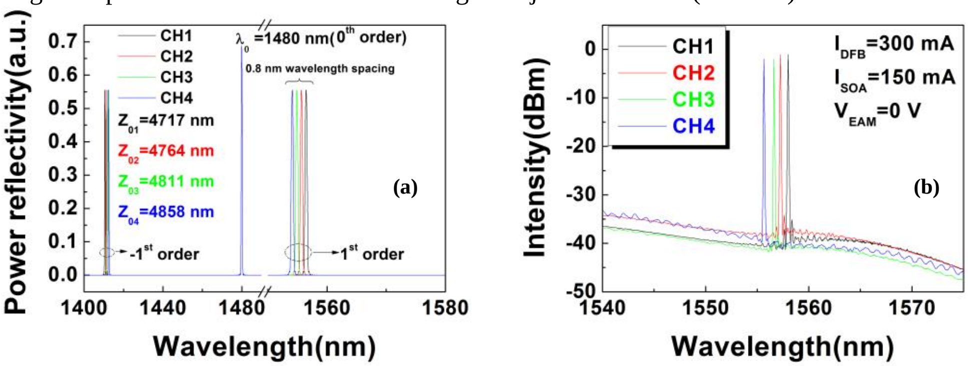

Fig. 2. (a) The simulated power reflectivity of the 0th and ±1st order granting of the four channels, (b) measured optical spectra of the four channels from SOA side when I_{DFB} = 300 mA, I_{SOA} =150 mA, and V_{EAM} = 0 V under 20°.

Fig. 3(a) shows the residual error of the four channel lasing wavelengths after linear fitting of the lasing wavelengths versus the channel number. The residuals vary from -0.084 to 0.13 nm. The residual value is reasonable and its variation is very small, which is due to the precise control of the grating period, Λ, and sampled grating periods, Z_0, offered by e-beam lithography. The residual can be eliminated either by tuning the drive current (by tuning the current by <10 mA out of 300 mA) or by slightly changing the temperature (<1.5 °C) using a separate heater in each channel (the temperature tuning coefficient is around 0.1 nm/K in the range 20-40 °C). Fig. 3(a) also shows the measured single-mode suppression ratios (SMSRs), which are >33 dB showing good SLM operation in the DWDM source. By comparing the spectra from the DFB and SOA sides, it was confirmed there was no degradation associated with the SOA. Fig. 3(b) shows the power coupled into single mode fiber (SMF) for the four channels when I_{DFB} =300 mA, I_{SOA}=150 mA. Because the coupling efficiency of the SMF is <30%, the true maximum output power from the SOA side is >10 mW. The residual output power at V_{EAM} = -4 V is the result of amplified spontaneous emission in the SOA. Because the loss associated with the 4×1 MMI coupler is 6 dB, using an arrayed waveguide grating (AWG) combiner instead would lead to an improvement in the direct current (DC) extinction ratio (ER).

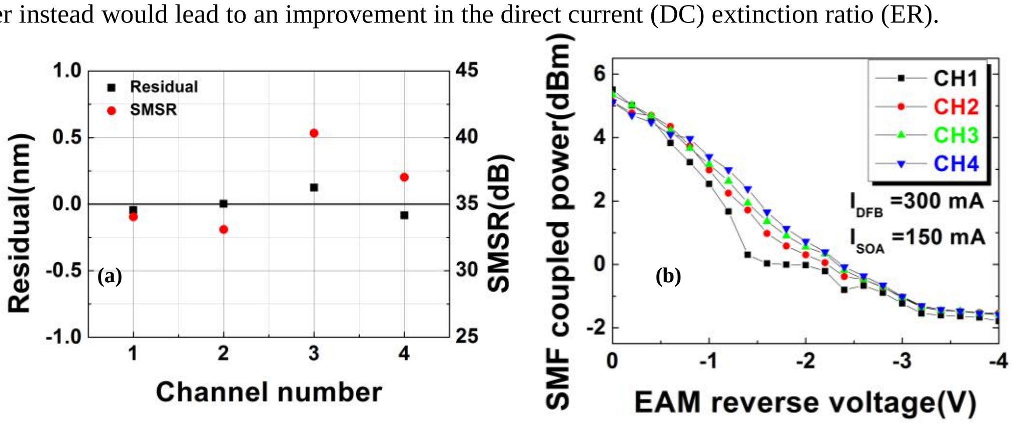

Fig. 3. (a) The residual of the lasing wavelength in Fig. 2(b) after linear fitting, (b) measured SMF coupled power of the four channels with I_{DFB} = 300 mA, I_{SOA} = 150 mA.

In conclusion, a DWDM source with a wavelength spacing of 0.8 nm has been demonstrated using the REC and QWI techniques, which have the advantage of giving precise control over the individual lasing wavelengths with a high SLM yield and eliminating the crystal re-growth that is required with traditional fabrication methods.

This work has been sponsored by the National Natural Science Foundation of China under grant no.61320106013 through a major international joint research program with UK

References

[1] H. Debrégeas-Sillard et al., C. R. Physique **9**, 1055 (2008).

[2] K. Kudo et al., IEEE Photon. Technol. Lett. **12**, 242 (2000).

[3] Y. C Shi et al., Scientific Reports. **4**, 7377 (2014).

[4] L. Hou et al., Photon. Technol. Lett. **23**, 1064-1066 (2011).